



Effect of Ta Doping on the Structural, Microstructural, and Electrical Properties of NaNbO_3 for Energy Storage Applications

Sairatun Nesa Soheli^{1,*}, Callum Wilson¹, Dongyang Sun¹, Islam Shyha¹ and Zhilun Lu²

¹School of Computing, Engineering and Built Environment, Edinburgh Napier University, Edinburgh EH10 5DT, United Kingdom

²School of Chemical and Process Engineering, University of Leeds, Leeds LS2 9JT, United Kingdom

Abstract

Enhancing the energy-storage performance of lead-free dielectric ceramics is essential for developing environmentally sustainable capacitors and power devices. NaNbO_3 , a promising perovskite, exhibits considerable potential for dielectric applications but is limited by poor densification and high dielectric loss. In this work, the effects of tantalum (Ta) doping at varying concentrations $\text{NaNb}_{1-x}\text{Ta}_x\text{O}_3$, with $x = 0.05, 0.10$, and 0.15 , corresponding to 5%, 10%, and 15% Ta substitution on the crystal structure, microstructure, and electrical properties of NaNbO_3 ceramics were systematically investigated. X-ray diffraction (XRD) confirmed phase purity and the orthorhombic perovskite structure, while scanning electron microscopy (SEM) revealed enhanced grain uniformity and densification with increasing Ta content. Electrical characterisation was conducted using complex impedance spectroscopy, dielectric loss ($\tan \delta$), capacitance (C'), and

admittance (Y') measurements over a frequency range of 10^1 to 10^6 Hz. The results indicate that 15% Ta-doped NaNbO_3 exhibits the optimal combination of a high dielectric constant and low dielectric loss. This improvement is attributed to refined grain morphology and optimised Ta substitution, confirming its potential as a high-performance, lead-free dielectric material for advanced energy-storage devices.

Keywords: NaNbO_3 , antiferroelectric, lead-free materials, perovskite ceramics, energy storage capacitors.

1 Introduction

The growing demand for efficient, reliable, and environmentally friendly power electronics has intensified research into lead-free dielectric energy storage materials [1, 2]. Among the promising candidates, NaNbO_3 has attracted significant attention as an antiferroelectric perovskite material, offering an exceptionally high Curie temperature (639°C), and versatile tunability of dielectric, electrical and energy storage properties through strategic



Submitted: 10 September 2025

Accepted: 05 November 2025

Published: 13 December 2025

Vol. 1, No. 1, 2025.

10.62762/JAEM.2025.415620

*Corresponding author:

✉ Sairatun Nesa Soheli

sairatunnesa.soheli@napier.ac.uk

Citation

Soheli, S. N., Wilson, C., Sun, D., Shyha, I., & Lu, Z. (2025). Effect of Ta Doping on the Structural, Microstructural, and Electrical Properties of NaNbO_3 for Energy Storage Applications. *Journal of Advanced Electronic Materials*, 1(1), 39–46.



© 2025 by the Authors. Published by Institute of Central Computation and Knowledge. This is an open access article under the CC BY license (<https://creativecommons.org/licenses/by/4.0/>).

chemical modification [3–5]. However, pure NaNbO_3 ceramics often suffer from issues such as poor densification, unstable dielectric behaviour, and high loss, limiting their practical applicability in energy storage applications [6–9]. To address these challenges, various doping strategies have been extensively utilised to increase electrical resistivity, enhance phase stability, and optimise energy storage performance. Tantalum (Ta^{5+}) is an effective dopant for modifying the structural and electrical behaviour of NaNbO_3 ceramics due to its ionic radius being comparable to that of Nb^{5+} , which enables easy B-site substitution in the perovskite lattice, and its significant impact on phase stability, polarisation mechanisms and dielectric response [10]. When Ta is incorporated into the NaNbO_3 lattice, it can introduce beneficial defect dipoles and induce local lattice distortions.

These effects may delay polarisation switching, typically leading to a reduction in the temperature-dependent dielectric permittivity peak while simultaneously lowering dielectric losses and enhancing breakdown strength [3]. Additionally, Ta doping affects grain growth dynamics and sintering behaviour, often resulting in enhanced microstructural uniformity and more controlled grain boundaries, which are important factors for achieving consistent dielectric performance and improved energy storage efficiency [10–13].

Recent studies have shown that the microstructure of dielectric ceramics, particularly grain size, morphology, and porosity, plays a critical role in governing the dielectric breakdown strength for high energy storage performance [14]. The maintenance of a single-phase perovskite structure is essential for achieving stable and reliable electrical properties under varying operating conditions. Furthermore, dielectric measurements such as relative permittivity (ϵ_r) and dielectric loss ($\tan \delta$) serve as indicators of a material's energy storage properties. High permittivity normally allows for larger polarisation, enabling greater energy density, while low dielectric loss minimises energy dissipation during charge-discharge cycles. An optimal balance of these properties, combined with favourable microstructural features, is essential for the development of next-generation dielectric materials for energy storage applications [11].

In this context, the present work investigates the effects of Ta doping at varying concentrations (5%, 10%, and 15%) on the crystal structure, microstructure, and

electrical properties of NaNbO_3 ceramics. Through comprehensive characterisation using XRD, SEM, and impedance spectroscopy, this study identifies an optimal Ta-doping level that shows potential for enhanced energy storage performance. The results provide valuable insight into structure–property relationships in lead-free dielectric systems and contribute to the advancement of sustainable materials for electrostatic energy storage applications.

2 Materials and Methods

Ta-doped NaNbO_3 ceramics with nominal compositions $\text{NaNb}_{1-x}\text{Ta}_x\text{O}_3$ ($x = 0.05, 0.10$, and 0.15) were synthesised via the solid-state reaction process. High-purity analytical-grade Na_2CO_3 (purity 99.8%), Nb_2O_5 (purity 99.99%), and Ta_2O_5 (purity 99.9%) powders served as the initial ingredients. Stoichiometric quantities were measured based on the desired compositions and ball-milled in isopropanol medium for 6 hours to achieve homogeneity. The dry powder mixtures were calcined at 900°C for 2 hours in air. Subsequently, the calcined powders were re-ground and milled as previously described. The re-milled powders were formed into disc-shaped pellets using polyvinyl alcohol (PVA) as a binder and heated at 600°C for 3 hours to remove the PVA, followed by sintering at 1350°C for 3 hours in air.

Phase purity and crystal structure were analysed using XRD within the 2θ range of 20° – 80° . The surface morphology and grain structure of sintered samples were examined using SEM. Electrical characterisation of Ta-doped NaNbO_3 ceramics was performed at room temperature over a broad frequency range (10^1 to 10^6 Hz). This evaluation included complex impedance spectroscopy to analyse resistive and capacitive behaviour, dielectric loss ($\tan \delta$) to assess energy dissipation, real part of capacitance (C') to quantify charge storage capability, and real part of admittance (Y') to examine conductive behaviour. Together, these techniques provide a comprehensive understanding of the materials' dielectric and electrical properties.

3 Results and Analysis

3.1 Structural Characterisation

Figure 1 shows the XRD patterns of Ta-doped NaNbO_3 ceramics with varying tantalum concentrations (5%, 10%, and 15%) after sintering. All diffraction peaks correspond to the orthorhombic perovskite structure of NaNbO_3 (ICDD Card No. 33-1270) [15], confirming

successful crystallisation without any secondary or impurity phases. This verifies that a single-phase perovskite structure was achieved for all compositions (5%, 10%, and 15% Ta), representing a key factor in ensuring stable dielectric performance. This result indicates that the synthesis route effectively produced phase-pure materials [16].

The diffraction peaks of the Ta-doped samples closely match those of undoped NaNbO_3 , confirming that Ta^{5+} ions were incorporated into Nb^{5+} lattice sites. A gradual shift of the diffraction peaks towards higher diffraction angles (2θ) with increasing Ta content is observed, attributed to the smaller ionic radius of Ta^{5+} (0.64 Å) compared with Nb^{5+} (0.69 Å), leading to slight lattice contraction consistent with Vegard's law.

The strong, sharp diffraction peaks reflect high crystallinity and low structural disorder, indicating that high temperature sintering promoted grain growth and densification. The absence of additional peaks, such as Ta_2O_5 or Nb_2O_5 , further confirms the chemical homogeneity of the doped samples.

Among the compositions, the 15% Ta-doped sample exhibits the sharpest diffraction peaks with the smallest full width at half maximum (FWHM), along with a systematic shift in 2θ positions toward higher angles. The reduced FWHM suggests enhanced crystallinity with fewer lattice distortions and defects, while the 2θ shift indicates lattice contraction due to the incorporation of Ta^{5+} ions. These structural modifications are expected to contribute to improved breakdown strength through reduced defect-mediated conduction pathways, lower dielectric loss, and consequently enhanced recoverable energy density. Therefore, the 15% Ta composition is considered the most promising for high-efficiency energy-storage applications.

3.2 Microstructural Analysis

Figure 2(a–f) shows the surface morphologies and grain-size distributions of Ta-doped NaNbO_3 ceramics containing 5%, 10%, and 15% Ta, observed using both secondary-electron (SE) and back-scattered-electron (BSE) modes at the same magnification (20 μm scale bar). Figure 2(a–c) display the SE micrographs together with their corresponding grain-size histograms, while Figures 2(d–f) show the complementary BSE images highlighting compositional contrast and phase uniformity. The histograms were obtained from ImageJ analysis based on the equivalent circular diameter (ECD) of

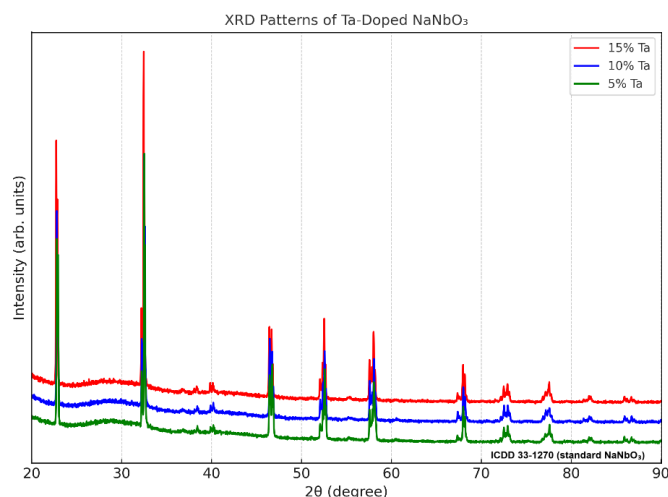


Figure 1. XRD patterns of Ta-doped NaNbO_3 ceramics (5%, 10%, and 15% Ta) after sintering, showing a single-phase orthorhombic perovskite structure referenced with the standard NaNbO_3 pattern (ICDD Card No. 33-1270) [15]. The reference peaks are indicated by vertical ticks at the bottom of the figure. The gradual peak shift toward higher 2θ values with increasing Ta content indicates lattice contraction and successful Ta incorporation..

individual grains.

In the case of 5% Ta doping in Figure 2(a, d) exhibits the microstructure consists of large, irregular grains interspersed with noticeable intergranular voids, suggesting incomplete grain coalescence during sintering. The histogram inset reveals a broad grain-size distribution with an average grain size of $7.6 \pm 3.3 \mu\text{m}$, indicating non-uniform grain growth and a relatively high population of oversized grains. Such heterogeneity weakens grain-boundary coupling, which can elevate leakage and diminish dielectric reliability. With 10% Ta incorporation shows in Figure 2(b, e), morphology becomes more uniform, characterised by well-fused, equiaxed grains with clearly defined boundaries and reduced porosity. The associated histogram displays a narrower, more symmetric distribution centered around $7.0 \pm 2.5 \mu\text{m}$, reflecting effective suppression of abnormal grain growth. This improved grain-size uniformity suggests enhanced densification and a more stable grain-boundary network, both beneficial for dielectric performance.

Upon further increasing the Ta content to 15% in Figure 2(c, f), the ceramic develops a densely packed, fine-grained microstructure with smooth interfaces and almost no observable porosity. The histogram confirms this trend, showing the finest and most concentrated distribution with an average grain size

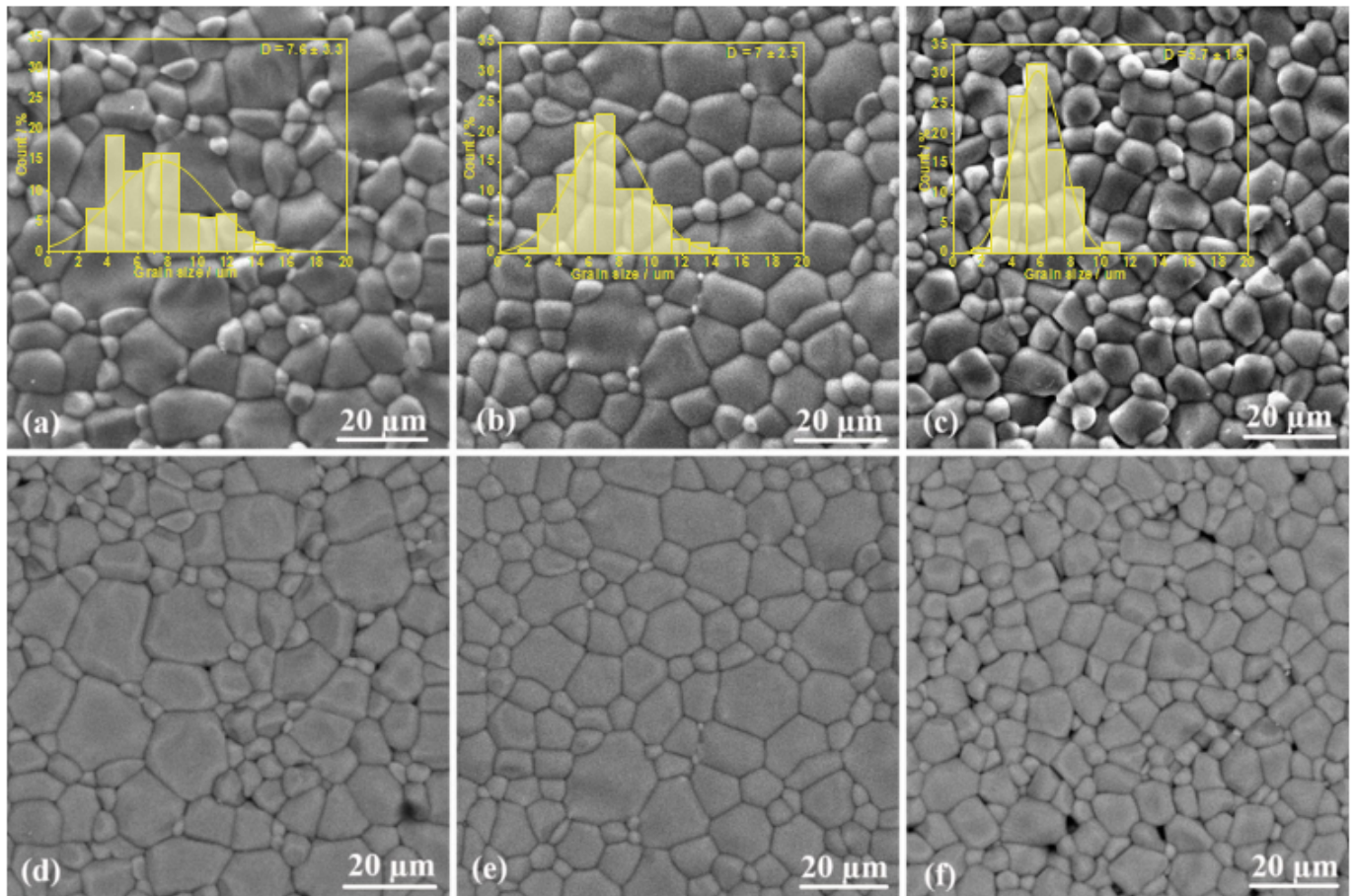


Figure 2. SEM micrographs and grain-size histograms of Ta-doped NaNbO_3 ceramics with different Ta contents: (a, d) 5% Ta, (b, e) 10% Ta, and (c, f) 15% Ta. Figures (a–c) show surface topography in SE mode with corresponding grain-size histograms, while Figures (d–f) display compositional contrast and phase uniformity in BSE mode. All images were captured at the same magnification (20 μm scale bar).

of $5.7 \pm 1.6 \mu\text{m}$. This pronounced refinement and uniformity indicate strong grain-boundary diffusion and compositional stability. The high boundary density in this composition contributes to defect suppression and electrical insulation, producing a microstructure highly favourable for dielectric applications.

Overall, progressive Ta doping from 5% to 15% produces grain refinement and improved homogeneity, as evidenced by the shifting and narrowing of the grain-size histograms. The decreasing average grain size and more compact distributions imply enhanced densification and controlled growth behaviour with increasing Ta content. Among all compositions, the 15 % Ta-doped sample exhibits the most uniform and defect-suppressed microstructure, indicative of superior structural integrity and dielectric reliability. The comparative influence of Ta doping on microstructure and energy-storage suitability is summarised in Table 1.

3.3 Electrical Analysis

The Nyquist plot (Z' vs. Z'') of Ta-doped NaNbO_3 ceramics Figure 3(a) reveal semicircular arcs whose diameters vary with Ta concentration. The 5% Ta-doped sample exhibits the largest semicircle, followed by 15% and 10% Ta. This indicates a higher bulk resistance and lower real part of admittance (Y') for 5% Ta-doped sample, suggesting reduced charge carrier mobility. However, a higher bulk resistance alone does not guarantee improved energy-storage performance. While the 5% Ta-doped sample shows the highest resistance, the 15% Ta-doped sample demonstrates a more favorable balance of moderate resistance, reduced dielectric loss, and enhanced capacitance—resulting in potentially higher recoverable energy density.

The variation of the dielectric loss tangent ($\tan \delta$) as a function of frequency for 5%, 10%, and 15% Ta-doped NaNbO_3 provides critical insight into the energy storage behaviour of these materials shown

Table 1. Effect of Ta Doping on microstructure and energy storage suitability.

Ta Doping Level	Figure Reference	Average Grain Size (μm)	Grain Morphology	Density & Porosity	Microstructure Uniformity	Energy Storage Suitability
5% Ta	2(a, d)	7.6 ± 3.3	Large, irregular grains with voids	High density, low porosity	Moderate	Moderate to Low – irregular structure, higher leakage
10% Ta	2(b, e)	7 ± 2.5	Well-fused equiaxed grains	High density, medium–low porosity	Good	High-refined, densified
15% Ta	2(c, f)	5.7 ± 1.6	Fine, compact grains	High density, negligible porosity	Excellent	Highest-defect-suppressed, stable microstructure

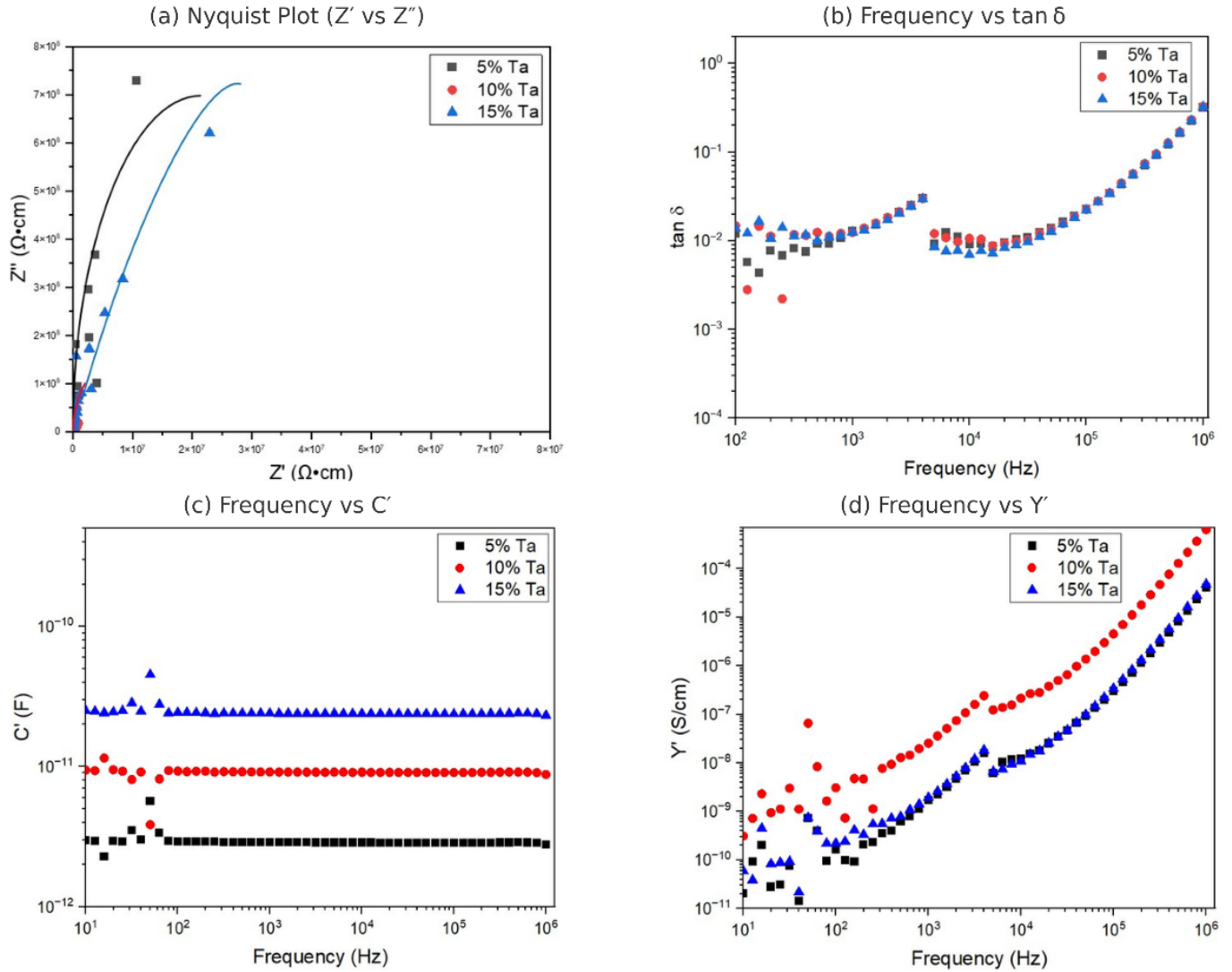


Figure 3. Electrical characterisation of Ta-doped NaNbO₃ ceramics: (a) Nyquist plot (Z'' vs. Z'), (b) frequency dependence of dielectric loss ($\tan \delta$), (c) real part of capacitance (C'), and (d) real part of admittance (Y') for 5%, 10%, and 15% Ta compositions.

in Figure 3(b). All compositions exhibit low $\tan \delta$ values (10^{-2} to 10^{-3}) across a broad frequency range, suggesting minimal energy dissipation, and favourable energy storage characteristics with high dielectric efficiency. At higher frequencies (above 10^4 Hz), all three samples exhibit a gradual rise in $\tan \delta$, which is typical of dielectric relaxation processes as the

polarisation mechanisms lag the applied field.

The variation of the real part of capacitance (C') with frequency in Figure 3(c) by 5%, 10%, and 15% Ta-doped NaNbO₃ provides critical insight into the materials' dielectric behaviour and energy storage potential. Across the frequency range C' , all

compositions display a characteristic trend where C' remains nearly constant after a slight initial fluctuation at very low frequencies. This plateau suggests a stable dielectric response, typical of grain-dominated polarisation mechanisms. Notably, the 15% Ta-doped sample exhibits the highest C' values throughout the entire frequency range, followed by the 10% and 5% Ta-doped samples, respectively. The higher capacitance observed in the 15% Ta-doped sample indicates a greater ability to store charge, which is advantageous for energy storage applications. This enhancement may be attributed to increased space charge polarisation or enhanced dielectric constant due to structural modifications introduced by higher Ta substitution. The 10% Ta sample also exhibits good capacitance values, while the 5% sample shows the lowest capacitance, indicating limited charge storage capability.

Figure 3(d) shows the frequency-dependent behaviour of the real part of admittance (Y') for 5%, 10%, and 15% Ta-doped NaNbO_3 ceramics provide key insights into the conductive and dielectric response of the materials. Across the frequency range of 10^2 to 10^6 Hz, all samples show an increasing trend in Y' , indicating enhanced charge mobility with rising frequency as the capacitive elements become more conductive. Notably, the 10% Ta-doped sample consistently exhibits the highest Y' values across nearly the entire frequency spectrum, peaking above 10^{-4} S/cm at high frequencies. Therefore, the 10% Ta-doped sample is more susceptible to breakdown due to its higher conductivity. The 15% and 5% Ta-doped sample both show low Y' values at lower frequencies, implying limited transport capability. At low frequencies, the Y' of all samples remains minimal due to interfacial polarisation and space-charge accumulation, which restricts current flow. As frequency increases, these resistive effects diminish.

Overall, the electrical characterisation demonstrates that Ta-doped NaNbO_3 ceramics achieve low dielectric loss, high resistivity, and stable capacitance across frequencies, which are highly desirable for energy storage applications. Although the 5% Ta-doped sample shows the largest semicircle in the Nyquist plot, indicating the highest bulk resistance, a higher bulk resistance does not necessarily correlate with superior energy storage behaviour. In dielectric systems such as Ta-doped NaNbO_3 , an optimal balance between moderate resistance, low dielectric loss, and high breakdown strength is more critical to achieving efficient charge storage and retrieval. The

15% Ta-doped sample therefore exhibits the most favourable combination of electrical characteristics, including enhanced insulation, high and stable capacitance, and low dielectric loss.

4 Summary

Based on comprehensive structural, microstructural, and electrical analyses, the 15% Ta-doped composition emerges as the most promising candidate for energy storage applications amongst the investigated doping levels. XRD results confirm that all samples retain a single-phase perovskite structure, with the 15% Ta sample exhibiting uniform peak shifts, confirming that Ta ions were incorporated into the lattice sites. SEM images reveal that this composition achieves the most homogeneous microstructure with the smallest grain size (see Figure 2), promoting effective domain alignment. Electrically, the 15% Ta sample demonstrates low conductivity and dielectric loss ($\tan \delta$) combined with the highest dielectric constant, signifying improved charge mobility and dielectric efficiency. These properties are particularly favourable for enhanced breakdown strength, which is crucial for superior energy storage performance. Therefore, the 15% Ta doping level offers the optimum balance between structural integrity, microstructural optimisation, and electrical performance. However, realising this potential depends on increasing the density of the 15% Ta-doped samples through optimised processing procedures, making it the most suitable formulation for advanced dielectric energy storage systems with further processing refinement.

Data Availability Statement

Data will be made available on request.

Funding

This work was supported without any funding.

Conflicts of Interest

The authors declare no conflicts of interest.

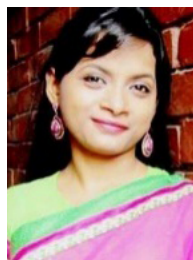
Ethical Approval and Consent to Participate

Not applicable.

References

- [1] Panda, P. (2009). Environmental friendly lead-free piezoelectric materials. *Journal of Materials Science*, 44(19), 5049–5062. [CrossRef]

- [2] Sun, Z., Wang, Z., Tian, Y., Wang, G., Wang, W., Yang, M., ... & Pu, Y. (2020). Progress, outlook, and challenges in lead-free energy-storage ferroelectrics. *Advanced Electronic Materials*, 6(1), 1900698. [CrossRef]
- [3] Yang, L., Kong, X., Li, Q., Lin, Y. H., Zhang, S., & Nan, C. W. (2022). Excellent energy storage properties achieved in sodium niobate-based relaxor ceramics through doping tantalum. *ACS Applied Materials & Interfaces*, 14(28), 32218-32226. [CrossRef]
- [4] Xu, M., Zeng, D., Wang, X., Nong, P., Pan, Y., Dong, Q., ... & Chen, X. (2023). Optimizing the energy storage performance of NaNbO₃ ceramics by rare-earth-based composite perovskite Sm (Mg_{0.5}Zr_{0.5}) O₃ modification. *Microstructures*, 3(4), N-A. [CrossRef]
- [5] Nain, R., & Dwivedi, R. (2023). Effect of tuning of charge defects by K, Ba, La doping on structural and electrical behaviour of NaNbO₃. *Materials Chemistry and Physics*, 306, 127999. [CrossRef]
- [6] Premwicheit, P., & Prasertpalichat, S. (2025). Structural, Dielectric, And Energy Storage Properties Of Ba₂+ Doped Lead-Free NaNbO₃-Based Ceramics. *Suranaree Journal of Science & Technology*, 32(1). [CrossRef]
- [7] Fan, Y., Zhou, Z., Liang, R., & Dong, X. (2019). Designing novel lead-free NaNbO₃-based ceramic with superior comprehensive energy storage and discharge properties for dielectric capacitor applications via relaxor strategy. *Journal of the European Ceramic Society*, 39(15), 4770-4777. [CrossRef]
- [8] Zhang, N., Zhu, M. M., Jia, P. P., Pan, Q. X., Zhang, X. M., Li, T., ... & Song, G. L. (2025). Boosting energy storage performance in NaNbO₃-based relaxor antiferroelectrics via structural refinement and domain modulation under moderate electric fields. *Ceramics International*. [CrossRef]
- [9] Liu, Z., Lu, T., Ye, J., Wang, G., Dong, X., Withers, R., & Liu, Y. (2018). Antiferroelectrics for energy storage applications: a review. *Advanced Materials Technologies*, 3(9), 1800111. [CrossRef]
- [10] Xiong, P., Tan, G. Q., & Ren, H. J. (2012). Influence of Ta⁵⁺ doping on the piezoelectric properties of KNN ceramics. *Key Engineering Materials*, 512, 1399-1402. [CrossRef]
- [11] Yang, W., Zeng, H., Yan, F., Lin, J., Ge, G., Cao, Y., ... & Zhai, J. (2022). Superior energy storage properties in NaNbO₃-based ceramics via synergistically optimizing domain and band structures. *Journal of Materials Chemistry A*, 10(21), 11613-11624. [CrossRef]
- [12] Zhao, M., Wu, W., Hui, J., Li, J., Wang, W., Du, C., ... & Jin, L. (2025). Advanced combination optimization tactics for enhancing the comprehensive energy storage performance of sodium niobate-based ceramic materials. *Journal of Materials Science: Materials in Electronics*, 36(32), 2078. [CrossRef]
- [13] Elaiyaraja, P., Karunakaran, N., Muralidharan, M., & Raj, S. G. (2025). Doping-induced structural, optical, and electrical modifications in (1-x) NaNbO₃-xBiGdKZrO₃ ceramics for microelectronic applications. *Journal of Materials Science: Materials in Electronics*, 36(12), 1-40. [CrossRef]
- [14] Soheli, S. N., Lu, Z., Sun, D., & Shyha, I. (2024). Lead-Free NaNbO₃-based Ceramics for Electrostatic Energy Storage Capacitors. *Ceramics*, 7(2), 712-734. [CrossRef]
- [15] International Centre for Diffraction Data. (n.d.). Powder Diffraction File – NaNbO₃ (ICDD Card No. 33-1270). Retrieved December 12, 2025, from <https://www.icdd.com>
- [16] Boukriba, M., Sediri, F., & Gharbi, N. (2013). Hydrothermal synthesis and electrical properties of NaNbO₃. *Materials Research Bulletin*, 48(2), 574-580. [CrossRef]



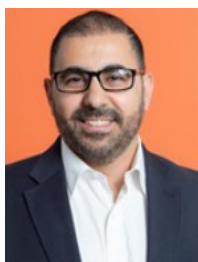
Sairatun Nesa Soheli is a Ph.D. researcher at Edinburgh Napier University, funded by a doctoral scholarship. She previously received the British Council Women in STEM Scholarship (2021) for her MSc at the same university. Currently on leave from her role as Assistant Professor in the EEE department at IUBAT, Bangladesh, she has over nine years of teaching experience. Her research focuses on lead-free antiferroelectric, dielectric, and piezoelectric ceramics, as well as cellulose materials, power electronics, and electrical systems. She has authored several peer-reviewed journal and conference publications. (Email: Sairatunnesa.Soheli@napier.ac.uk)



Dr Callum Wilson has a background in materials engineering, and over the past number of years has been involved in the design and implementation of several high-profile projects which demonstrated fuel cell and other low carbon energy systems in real world applications. In recent years, Callum has been part of several teams at Edinburgh Napier University that have been developing novel material technologies for use within the Energy, Fuel Cell, Oil & Gas and Specialist Coatings fields. He has extensive industrial engineering experience, has undertaken more than 20 major consultancies and is a professional member of the Institute of Materials, Minerals and Mining. (Email: C.Wilson3@napier.ac.uk)



Dr Dongyang Sun is a Lecturer of the School of Computing Engineering and the Built Environment at Edinburgh Napier University. He has obtained a lot of experience with cellulose and cellulose processing. His expertise includes knowledge on scanning/transmission electron microscopy, nanomaterials processing and characterisation techniques including XRD, TGA-DSC, EDXA, AFM, FTIR, UV-Vis. He has also been working on the swelling behaviour of various wood species, for example using dynamic vapour sorption apparatus. He is the co-author in some publications of peer-reviewed journals in the relevant subject areas. (Email: D.Sun@napier.ac.uk)



Prof. Islam Shyha is a Professor of Manufacturing Engineering in the School of Computing, Engineering and the Built Environment, Edinburgh Napier University. Prof. Shyha received his Postgraduate Certificate in Higher Education Practice from Northumbria University, PhD from The University of Birmingham, MSc, and BSc from Alexandria University. Prof. Shyha has been awarded several research projects funded by

Newton Fund, Innovate UK, and industrial organisations. He teaches mechanical and manufacturing engineering courses and supervises MSc and PhD projects in advanced manufacturing and materials. (Email: I.Shyha@napier.ac.uk)



Dr Zhilun Lu is an Assistant Professor of Materials Science and Engineering at University of Leeds. His research group focuses on the structure-composition property relations of a broad spectrum of advanced functional materials, particularly ferroelectrics and thermoelectric. His expertise lies in employing impedance spectroscopy to probe electrical properties and neutron scattering to elucidate atomic structure and dynamics. He

has led projects funded by the Royal Society and Royal Society of Chemistry. He is a frequent invited speaker at international conferences and serves on the editorial boards of several top materials science journals. (Email: Z.Lu@leeds.ac.uk)